Journal of Hazardous Materials 465 (2024) 133093

Contents lists available at ScienceDirect

Journal of Hazardous Materials

journal homepage: www.elsevier.com/locate/jhazmat

Research Paper

Tritiated stainless steel (nano)particle release following a nuclear dismantling incident scenario: Significant exposure of freshwater ecosystem benthic zone

Danielle L. Slomberg [a,*], Mélanie Auffan [a,b], Mickaël Payet [c], Andrea Carboni [a], Amazigh Ouaksel [a], Lenka Brousset [d], Bernard Angeletti [a], Christian Grisolia [c], Alain Thiéry [d], Jérôme Rose [a,b]

[a] CNRS, Aix-Marseille Univ., IRD, INRAE, CEREGE, 13545 Aix-en-Provence, France
[b] Civil and Environmental Engineering Department, Duke University, Durham, NC 27707, United States
[c] CEA, IRFM, F-13108 Saint-Paul-lez-Durance, France
[d] CNRS, IRD, IMBE, Aix-Marseille Univ, Avignon Univ., Marseille, France

HIGHLIGHTS

- Tritiated (nano)particles may release during nuclear decommissioning incident.
- No stainless steel particle dissolution, 100% accumulation in aqueous sediments.
- Majority of tritium (>80%) remains associated to stainless steel (nano) particles.
- *A. vortex* exhibit burrowing behavioral change despite no acute particle toxicity.

GRAPHICAL ABSTRACT

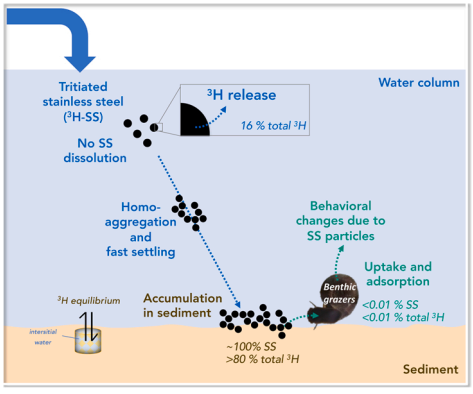

ARTICLE INFO

Editor: Lingxin CHEN

Keywords:
Stainless steel particles
Tritium
Nuclear reactor dismantling
Aquatic mesocosm
Environmental exposure
Ecotoxicity

ABSTRACT

Nuclear facilities continue to be developed to help meet global energy demands while reducing fossil fuel use. However, an incident during the dismantling of these facilities could accidentally release tritiated particles (e.g. stainless steel) into the environment. Herein, we investigated the environmental dosimetry, fate, and impact of tritiated stainless steel (nano)particles (1 mg.L^{-1} particles and 1 MBq.L^{-1} tritium) using indoor freshwater aquatic mesocosms to mimic a pond ecosystem. The tritium (bio)distribution and particle fate and (bio)transformation were monitored in the different environmental compartments over 4 weeks using beta counting and chemical analysis. Impacts on picoplanktonic and picobenthic communities, and the benthic freshwater snail, *Anisus vortex,* were assessed as indicators of environmental health. Following contamination, some tritium (~16%) desorbed into the water column while the particles rapidly settled onto the sediment. After 4 weeks, the

* Corresponding author.
E-mail address: slomberg@cerege.fr (D.L. Slomberg).

https://doi.org/10.1016/j.jhazmat.2023.133093
Received 24 July 2023; Received in revised form 7 November 2023; Accepted 23 November 2023
Available online 29 November 2023

Radiotoxicity
Sediment accumulation

particles and the majority of the tritium (>80%) had accumulated in the sediment, indicating a high exposure of the benthic ecological niche. Indeed, the benthic grazers presented significant behavioral changes despite low steel uptake (<0.01%). These results provide knowledge on the potential environmental impacts of incidental tritiated (nano)particles, which will allow for improved hazard and risk management.

1. Introduction

Natural nanoparticles or colloids (from natural mineral weathering, ocean spray, volcanoes, etc.) have been known to be involved in the transport of pollutants in surface and groundwaters for decades. Indeed, in 1989, McCarthy and Zachara first called attention to "the potentially critical, but poorly understood role of colloids in facilitating contaminant transport," with a particular emphasis on the transport of radionuclides [1]. Since then, a large number of studies have focused on the mechanisms, thermodynamics, and kinetics of the bio-physico-chemical interactions between these natural nanoparticles and a variety of pollutants (e.g. metals, metalloids, radionuclides, organics) [2–5].

In recent years, another source of nanoparticles in the environment has been identified, resulting from the release of incidental, anthropogenic nanoparticles formed due to processes such as combustion, wear, corrosion, and abrasion over the course of a material's lifecycle [6]. In the case of nuclear energy facilities, incidental nanoparticles can be produced during routine reactor operation and maintenance (e.g. tungsten nanoparticles) [7,8], and decommissioning phases (e.g. stainless steel and cement) [9]. Under normal operating and decommissioning conditions, these particles are contained due to the use of ventilation systems equipped with High Efficiency Particulate Air (HEPA) filters [10]. However, in the case of a containment system failure, such incidental nanoparticles could be subsequently released into the environment and their environmental behavior, fate, hazard, and role in vectorizing radioactive contaminants such as tritium still requires investigation [11].

Tritium (^{3}H), present in nuclear reactors as a by-product or reaction source, is a highly mobile, radioactive isotope of hydrogen (half-life of 12.3 years) and has already been shown to be radiotoxic in the environment [12–15]. Tritium easily exchanges with water to form tritiated water, and can also bind to carbon chains of organic molecules [14,16–18]. The organic complexation of tritium is known to enhance its bioaccumulation in the environment and favor its trophic transfer [19]. Tritium can also be adsorbed at the surface of natural nanoparticles where it substitutes the protons of the structural hydroxyls [20]. As previously mentioned, radionuclide adsorption onto natural nanoparticles is a well-known mechanism controlling their transport and migration in surface and groundwaters [21,22]. However, many gaps remain in understanding how tritium association with or transport by incidental, anthropogenic nanoparticles generated during dismantling activities will impact its environmental behavior and fate [9].

As such, tritiated stainless steel (nano)particles, which may be incidentally emitted into freshwater environments during decommissioning activities, were selected as the focus for this study. Once released into aquatic ecosystems, these particles may release constituting metals (e.g. Cr, Ni, Mo, Fe) and tritium into the water column. They may also agglomerate and settle down due to their density (i.e. 7900 kg.m^{-3}) and an isoelectric point at the environmentally relevant pH of 7.8 [23,24]. To date, little is known about the behavior, fate and toxicity of such incidental tritiated stainless steel (nano)particles and it is therefore difficult to anticipate the effects of an accidental release. Previous studies have assessed the ecotoxicity of metallic and metal oxide-based nanoparticles (e.g. Ag, Au, CuO, ZnO, CeO_2) towards aquatic invertebrates (e.g. bivalves, gastropods, crustaceans) and demonstrated that these nanoparticles can increase reactive oxygen species (ROS) production and lead to toxicity [25,26]. The possibility for nanoparticles to cross biological barriers and accumulate in aquatic organisms has also been linked to toxicity [27]. Based on this knowledge, any stainless steel (nano)particle toxicity will likely be related to particle solubility and/or the ability to bioaccumulate in organisms. Vernon et al. [28] reported a lack of genotoxicity and low accumulation in the marine filter feeders *Mytilus galloprovincialis* exposed to 1 mg.L^{-1} stainless steel (nano)particles (non-radioactive) under controlled conditions. However, there have been no prior studies on the impacts of stainless steel (nano)particles to freshwater organisms. In addition, further work employing radioactive tritiated stainless steel (nano)particles has yet to be completed to elucidate the potential combined impacts.

Depending on the physico-chemical properties and transformations of the tritiated stainless steel (nano)particles in natural environments, the organisms and ecological niches likely to be exposed will differ (e.g. benthic versus planktonic compartments, filter-feeders versus benthic grazers, primary producers versus consumers). Moreover, the presence of dissolved ions and natural suspended matter in natural environments must be taken into account, as they will strongly modify tritiated stainless steel (nano)particle behavior and fate [29–31]. To date, the main limitation for a better assessment of the behavior of tritium associated to or transported by incidental nanoparticles (e.g. stainless steel) is the difficulty in monitoring their behavior and fate in complex and relevant environmental matrices (e.g. sediment, biota). Due to their nanometric size and heterogeneous distribution, it remains challenging to link macroscopic effects (e.g. ecotoxicity, distribution within organisms) to the evolution of the particle's nanometric properties (e.g. surface adsorption/desorption, homo/hetero-aggregation) in a relevant exposure scenario [32]. To this end, aquatic mesocosms are an invaluable experimental tool due to their ability to mimic realistic contamination scenarios (e.g. low doses) that account for the complexity and synergies between contaminants and natural components, while allowing for the monitoring of multiple endpoints and the investigation of the impacts on several ecological niches [33,34].

Herein, we investigated the environmental dosimetry, fate, and impact of tritiated stainless steel (nano)particles on a pond ecosystem under static conditions using indoor freshwater aquatic mesocosms designed to simulate a one-time contamination following a dismantling incident scenario. The contamination was performed by injecting tritiated stainless steel particles (or hydrogenated stainless steel particles as a non-radioactive control) into the mesocosm for a final concentration of 1 mg.L^{-1} incidental (nano)particles and 1 MBq.L^{-1} tritium. The tritium (bio)distribution and stainless steel particle fate and (bio)transformation were monitored in the different environmental compartments (e.g., water, sediment, biota) over 4 weeks, using beta counting and chemical analysis, respectively. Impacts on picoplanktonic and picobenthic communities, as well as the benthic grazer gastropod, *Anisus vortex*, were assessed as indicators of environmental health. Through these investigations, our goal was to provide some of the first key knowledge on the environmental impacts of radiocontaminants associated to or transported by incidental (nano)particles from the nuclear energy sector, which will be crucial for improving hazard and risk management.

2. Materials and methods

2.1. Aquatic mesocosm set-up

For each experiment (i.e., radioactive and non-radioactive), four indoor aquatic mesocosms (glass tanks of 350 × 200 × 400 mm) were set up to mimic a natural pond ecosystem. The organisms selected for this study were picoplankton and picobenthos primary producers (e.g., bacteria, algae, protozoa from natural inoculum) and the benthic

grazing snail, *Anisus vortex* (L., 1758), sampled from a non-contaminated pond in the South of France (N 43°20′47.04″, E 6°15′34.786″). The pond physical-chemical parameters on the field sampling day were: electrical conductivity = 432 µS.cm^{-1}, temperature = 11 °C, pH = 8.1, dissolved O_2 = 8.6 mg.L^{-1} (94% of saturation), and total dry residue (organic and mineral) = 280 mg.L^{-1}.

Each mesocosm consisted of a bottom layer of ~2.3 kg artificial sediment (89% SiO_2, 10% kaolinite, and 1% $CaCO_3$) covered by 150 g of water-saturated natural sediment containing primary producers (sieved at 250 µm), followed by 16 L of Volvic® water, which has pH and conductivity values close to those of the natural pond water. Picoplankton recovered from the natural pond surface water were also added to the mesocosm. Briefly, 100 mL of pond water was sieved (250 µm), then successively filtered at 2 µm and 0.2 µm. The 0.2 µm filter was then recovered and agitated in 100 mL Volvic® water to resuspend the picoplankton, and 40 mL of this water inoculum was injected into each mesocosm. A day/night cycle of 6 h/18 h was applied using full spectrum light (Viva® light T8 tubes 18 W), and the room temperature ranged between 16.0 ± 1.5 °C. The mesocosm experiments were performed under static conditions, with no pumping or water circulation. Ultrapure water was added to the mesocosms weekly to compensate for evaporation. Two weeks of equilibration were necessary for the stabilization of the mesocosm physico-chemical parameters and the development of the primary producers. Then, ~20 adult *A. vortex* (6.0 ± 0.6 mm diameter) were introduced per mesocosm and acclimatized for 3 days prior to starting the experiment. More information on the experimental procedure can be found in Auffan et al [35].

2.2. Tritiated and hydrogenated stainless steel particles

Commercial stainless steel (SS316L, Product No. FF216030) particles with a main elemental composition of 69% *w/w* Fe, 17% *w/w* Cr, 10% *w/w* Ni, 2% *w/w* Mo, 1.4% w/w Mn, were purchased from Goodfellow® (Huntingdon, England). These commercial stainless steel particles were selected based on parameters defined from preliminary work in which particles were produced from a stainless steel rod by saw cutting [36]. The process used to label the stainless steel particles is based on thermally activated diffusion. Tritiated stainless steel (nano)particles (T-SS) were obtained using a three-step procedure developed at CEA Saclay (French Alternative Energies and Atomic Energy Commission): i) the commercial SS316L particles were first treated two times at 450 °C for 2 h under high pressure (1.2 ×10^5 and 1.4 ×10^5 Pa, respectively) with $^1H_2$ in order to stabilize the surface of the particles in a reducing atmosphere; ii) during the second treatment the particles were exposed to tritium gas ($^3H_2$) at 450 °C and 1 × 10^5 Pa; and iii) to complete the process, a degassing step was performed to eliminate any mobile tritium, which resulted in a T-SS particle specific radioactivity of 1 MBq.mg^{-1} [37]. This specific activity is proportional to the content of tritium trapped in the material (bound or unbound). The stability of the T-SS particles with respect to the tritium content was confirmed by measuring the specific activity before and after 3 months of storage in a glovebox in air. A batch experiment was also conducted to determine the short-term tritium release kinetics in abiotic mesocosm water (i.e. Volvic®) using the same T-SS particle concentration to be introduced in the mesocosms (i.e., 1 mg.L^{-1}). Briefly, a 1 mg.L^{-1} suspension of T-SS (10 mL) was prepared in Volvic® water and stirred continuously. This suspension was sampled (2 mL) at 1, 3, 6, 48, and 92 h. Each aliquot was immediately filtered by centrifugation (4000xg for 1 h) using Amicon® Ultra-4 3 K centrifugal filter devices (3 000MWCO, size retention limit ~ 1 nm, Merck-Millipore®) and the filtrate (i.e., dissolved fraction) was measured directly by liquid scintillation counting (Tri-Carb 2910TR analyzer, Perkin Elmer). The % tritium (^3H) release was determined using the ratio of the volumetric release activity to the initial volumetric activity.

Surrogate, hydrogenated stainless steel (nano)particles (H-SS) were also prepared as a non-radioactive control and were obtained by exposing the commercial particles to the same temperature and pressure conditions, but using $^1H_2$ instead of $^3H_2$ for the second step at 450 °C and 1 × 10^5 Pa. The H-SS particles were characterized for size, morphology, elemental composition, and crystalline phases using scanning electron microscopy (SEM) with Energy Dispersive Spectroscopy (EDS) analysis, optical particle counting, and X-ray diffraction (XRD), as detailed in Experimental S1 and as shown in Fig. 1. Of note, the treatment process used to obtain the H-SS particles did not result in any significant change in size, morphology, or elemental composition. The average SEM size for the pristine commercial particles was 1.72 ± 1.14 µm, with 2 particle populations centered around ~0.7 µm and ~4 µm, while for the H-SS particles the average SEM size was 1.73 ± 0.99 µm with 2 particle populations centered around ~0.8 µm and ~3 µm (Fig. S1). Furthermore, these SEM size distributions were coherent with those obtained via optical particle counting in ultrapure and Volvic® water (Fig. 1).

2.3. Particle exposure scenario of a lentic ecosystem

The aquatic mesocosm experiments were designed to simulate a one-time contamination of a pond ecosystem under static conditions with tritiated steel particles (Fig. 2). Stainless steel fate and behavior in the mesocosms was monitored at the CEREGE using the surrogate H-SS particles, while tritium distribution in the different environmental compartments was determined using T-SS particles in a parallel experiment conducted at the Saclay tritium lab (CEA). The one-time contamination was performed by injecting 16 mL of a suspension (in ultrapure water) containing 16 mg of H-SS or T-SS for a final concentration of 1 mg.L^{-1} stainless steel particles in the mesocosm water column. In the case of the T-SS exposure, the injection of 1 mg.L^{-1} T-SS corresponded to a tritium concentration of 1 MBq.L^{-1} i.e., 1 MBq per mg of SS. Of note, due to the need to limit the production and management of tritiated waste, the aquatic mesocosms exposed to T-SS particles were used to obtain tritium concentrations in the different environmental compartments (i.e. sediment, biota, water column), as well as a qualitative assessment of ecosystem stability following exposure. All other monitoring and sampling procedures described below were conducted using the non-radioactive, surrogate aquatic mesocosms.

2.4. Aquatic mesocosm monitoring

For each mesocosm, multiparameter probes (Odeon® Open X) were installed (~20 cm below the air-water interface and 7 cm above the sediment) to monitor the temperature (°C ± 0.5 °C), pH (unit ± 0.1 unit), redox potential (mV ± 1 mV), electrical conductivity (µS/cm ± 2 µS/cm), and dissolved O_2 (mg.L^{-1} ± 0.1 mg.L^{-1}) in the water column for the entire duration of the experiment. The number of colloidal particles suspended in the water column was monitored weekly at 10 cm below the water surface using an optical particle counter (Flowcell FC200S + HR, Occhio®, Belgium). Particles with sizes ranging from 0.2 to 52 µm in the water column were considered.

2.5. Organism viability and behavior

Picobenthos and picoplankton (cells between 0.2 and 2 µm) concentrations were determined at the surface of the sediment (0.5 ± 0.1 mm depth) and in the water column (10 cm below the air-water interface) on a weekly basis. To determine picoplankton concentrations, water (10 mL) and sediment (15 mL) were sampled at days 0 and 28, treated with formaldehyde (3.7%), and stored at 4 °C until counting. Counting was performed by mixing 10 µL of each sample with 5 µL 3 µM SYTO® 9 Green Fluorescent Nucleic Acid Stain on a glass slide and observing the number of cells in five different zones using a fluorescence microscope. The concentration of picoplankton (cells.mL^{-1}) was reported as the mean ± standard deviation of the five different zones. The benthic grazing snail, *A. vortex*, was observed weekly for viability and localization within the mesocosm (i.e., at the water surface or in the sediment) as an indication of potential behavioral changes. These

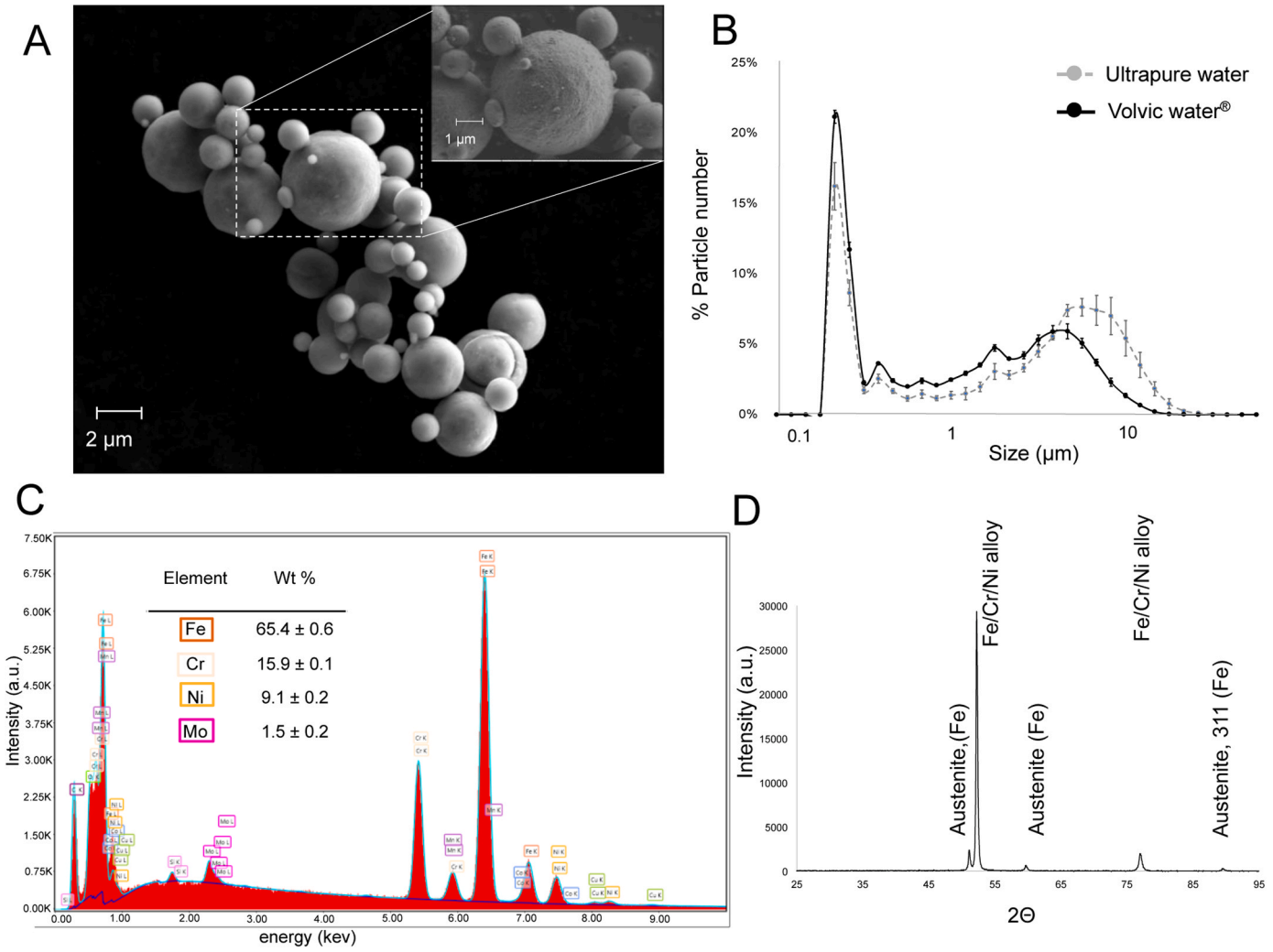

Fig. 1. Hydrogenated SS particle characterization: A) SEM image (EHT = 15 kV, WD = 12.5 mm, BSD4A, Mag. = 3.39 kX), B) optical counter size distribution analysis in ultrapure and Volvic® water (0.5 $g.L^{-1}$), C) Elemental composition based on EDS analysis, and D) XRD diffractogram (λ_{Co} = 1.79 Å).

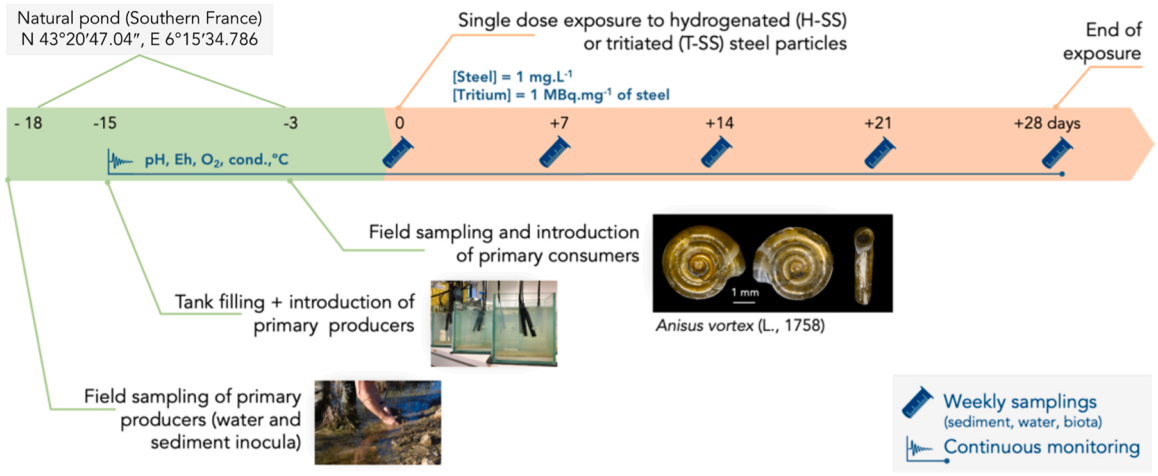

Fig. 2. Schematic of the set-up, sampling, and monitoring of the freshwater indoor mesocosm experiments performed in the Tritium lab in CEA Saclay (France) and the CEREGE mesocosm facilities (France).

behavioral changes are considered as a short time response and are both ecologically relevant and sensitive to environmental stressors [38,39].

2.6. Tritium and SS particle quantification in different environmental compartments of lentic ecosystem

The tritium and the SS particle distributions in the mesocosms were quantified by respectively measuring the tritium and main stainless steel metals (i.e., Fe, Cr, Ni, Mo, Mn), in the surficial sediments, water column, and the *A. vortex* organisms. Sampling was performed weekly over 4 weeks (i.e. Days 0, 7, 14, 21 and 28). The surficial sediments were sampled at three different locations and then pooled before drying 24 h at 50 °C. The estimated depth sampled using this procedure was 0.32 ± 0.07 cm below the water /sediment interface. The water column (10 mL) was sampled with a pipette at 10 cm below the surface of the water. The soluble fraction of the water column was also collected for tritium and metal analysis by sampling aliquots of surface water (4 mL) at the same depth and centrifuging them in Amicon® Ultra-4 3 kDa centrifugal filter devices (3000 MWCO, size retention limit ~ 1 nm, Merck-Millipore®) at 4000xg for 1 h to separate the soluble and particulate fractions. Concerning the benthic organisms, ten *A. vortex* were sampled at weeks 2 and 4, rinsed with clean Volvic® water (3 mL), and stored after drying 24 h at 50 °C.

Concerning the radioactivity (i.e. tritium) measurements, liquid scintillation counting was performed using a Tri-Carb 2910TR analyzer from Perkin Elmer. Two types of measurements were performed, either a direct measurement in the case of water samples, or after acid digestion in the case of the solid samples (i.e. surficial sediments and *A. vortex*). The solid samples were analyzed after drying (24 h at 50 °C), grinding, and acid digestion (3 volumes of 37% HCl Normatom® and 1 vol of 65% HNO_3 Normatom® for 48 h). The resulting solution contained a high concentration of ions and the particle digestion induced a coloration of the solution. The digestion solution was therefore diluted with 3 volumes of ultrapure water before measurement to limit quenching effects during liquid scintillation counting.

Before ICP-MS elemental analysis for metal content, the water column and *A. vortex* rinse samples (2 mL) were acid-digested at ambient temperature (3 mL 37% HCl Normatom® + 1 mL 65% HNO_3 Normatom®) for 48 h. Sediment and *A. vortex* samples were first ground using a mortar and pestle, then mineralized at 180 °C by using a microwave digestion system (ultraWAVE, Milestone, Italy) prior to ICP-MS analysis. For elemental analysis of sediment samples (50 mg), a mixture of 3 acids (1.5 mL HCl 37% (Normatom®), 1 mL HNO_3 65%, 1 mL of HF 47%− 51%) was used, while *A. vortex* organisms (50 mg) were digested in 1 mL HCl 37%, 1 mL HNO_3 65%, 1 mL H_2O_2 30%− 32% (PlasmaPure®) and 0.5 mL HF 47%− 51%. All digested residues were diluted to 10 mL with ultrapure water before analysis of Fe, Cr, Ni, Mo, and Mn concentrations using a PerkinElmer NexION 300X quadrupole ICP-MS.

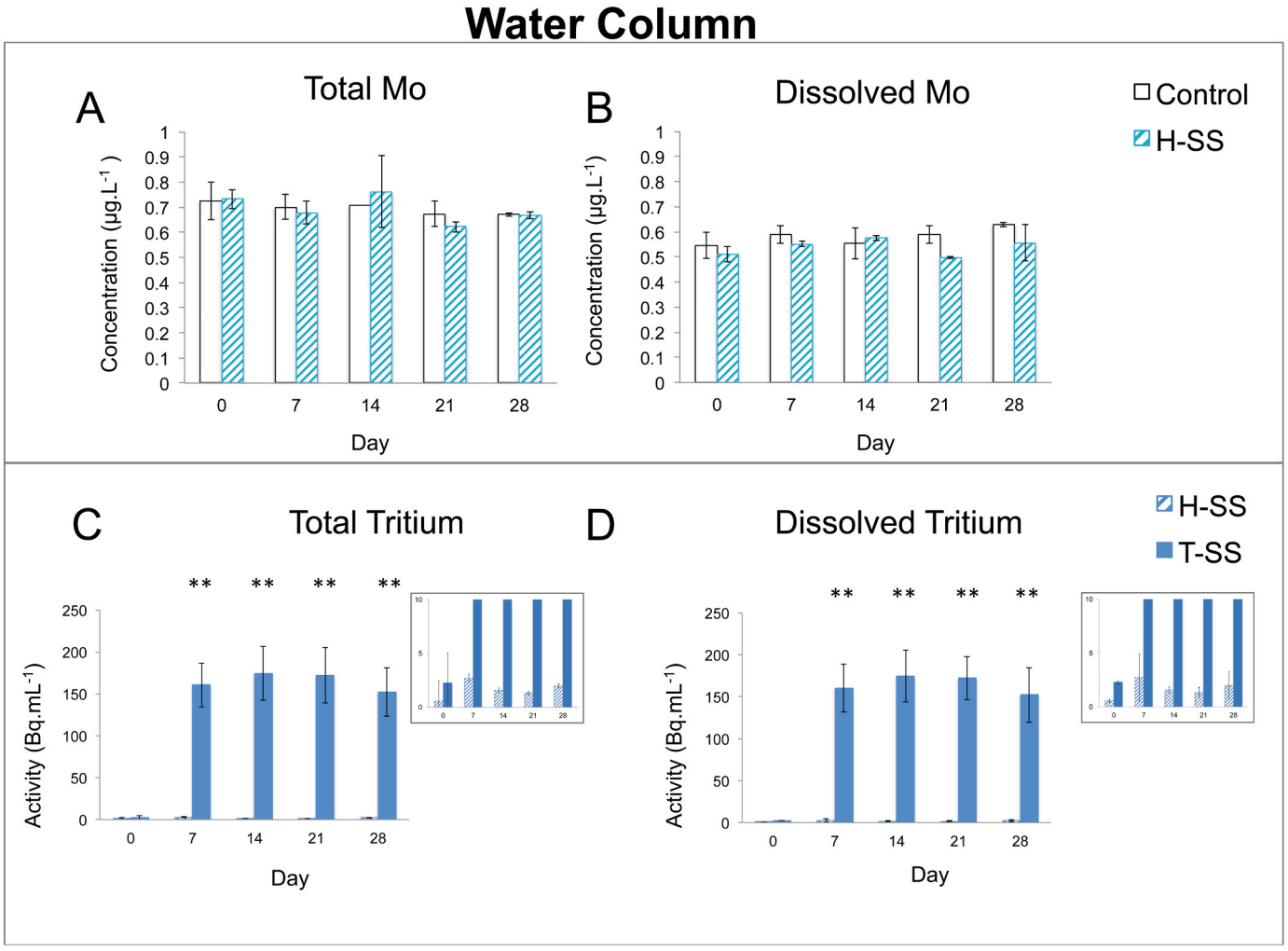

Fig. 3. (A) Total Mo concentration ($\mu g.L^{-1}$) and (B) dissolved Mo concentration ($\mu g.L^{-1}$) in the water column of the control and H-SS exposed mesocosms. (C) Total ^3H activity ($Bq.mL^{-1}$) and (D) dissolved ^3H activity ($Bq.mL^{-1}$) in the water column of the H-SS and T-SS exposed mesocosms. Statistical differences between exposed and control mesocosms were evaluated with the Student's t-test; * * $p < 0.05$.

Although the main elements (i.e., Fe, Cr, Ni, Mo, Mn) comprising the SS particles were quantified in each environmental compartment (i.e., water column, surficial sediment, and primary consumers), not all elements could be used as tracers due to high background concentrations (Experimental S2 and Fig. S4). Three elements (i.e., Cr, Ni, and Mo) were found to be suitable as tracers of the SS particles (Figures SI). For clarity, only the data associated with using Mo as a tracer of SS in water and sediment is presented, however comparable results which support the same conclusions were obtained using Cr and Ni as tracers (Figs. S5 & S7).

3. Results and discussion

3.1. Tritiated stainless steel particle fate, behavior, and impacts in the planktonic compartment

3.3.1. Tritium and SS behavior and fate in the water column

Fig. 3A & 3B show the Mo concentrations (tracer of SS particles) measured in the water column as a function of time. No significant increase in either the total Mo concentration (~0.6–0.7 $\mu g.L^{-1}$) or the dissolved Mo concentration (~0.5–0.6 $\mu g.L^{-1}$) was observed in the water column of mesocosms contaminated with H-SS during the one-month experiment. This highlights the fast kinetics of SS particle removal from the water column that occurred during the first week. The lack of an increase in Mo concentration in the dissolved fraction over the entire experiment duration is consistent with the slow dissolution kinetics of SS. The negligible SS solubility was further confirmed by the lack of other SS metals (i.e. Cr and Ni) being released into the dissolved phase (Fig. S5).

Fig. 3C gives the tritium activity in the water column following exposure to T-SS. Seven days after contamination significant tritium activity was measured in the water column, which remained stable over time. The ~150 $Bq.mL^{-1}$ measured in the water column corresponded to 16 ± 2% of the total tritium injected. To identify whether the tritium was bound to particles (SS or natural suspended particles) or dissolved, ^{3}H activity was also measured after ultrafiltration of the water at 3 kDa. The similar tritium activities measured before and after ultrafiltration allowed us to conclude that the tritium measured in the water column of the mesocosms was fully dissolved (Fig. 3D).

Understanding the distribution of tritium between the stainless steel surface, near surface, and bulk metal is necessary for determining how the tritium is released from the T-SS particles in freshwater ecosystems. Matsuyama et al. [40] suggested that the tritium atoms trapped by oxidized layers at the SS surface easily react with water molecules and are quickly released in water at ambient temperature. We evaluated the short-term release kinetics of ^{3}H release using a batch experiment and estimated that 12 ± 1.5% of the total ^{3}H is released after 48 h (Fig. S6). Thereafter, the ^{3}H release did not change significantly up to 92 h (14 ± 1% ^{3}H release) or even after 28 days (16 ± 2%) in the mesocosms, which indicates that a quasi-equilibrium state had been reached [41].

3.3.2. Homo-aggregation versus hetero-aggregation of tritiated steel particles

Two mechanisms can be involved in the fast removal of SS from the water column and their settling at the surface of the sediment: homo-aggregation between SS particles and/or hetero-aggregation with natural colloids. Indeed, natural colloids present in the mesocosm water (e.g. suspended clays, natural organic matter) can cause the formation and settling down of hetero-aggregates [27]. In the mesocosm water, the number of colloids in the 0.2–1 μm fraction (mostly kaolinite clay) was close to 10^{5} $particles.mL^{-1}$ (Fig. 4). No significant differences in the number of colloids were observed after steel particle injection, indicating that hetero-aggregation was not predominant under these experimental conditions.

Moreover, because of the pH and ionic strength of the mesocosm water column, SS particles are colloidally unstable and will likely homo-aggregate [22,23]. Using Stokes' law the particle sedimentation velocity can be calculated: [42].

$$\nu = \frac{2}{9}\frac{(\rho p - \rho f)}{\mu} g R^{2}$$

where v is the velocity ($m.s^{-1}$), g the gravitational field strength ($m.s^{-2}$), R the radius of the spherical particle (m), ρ_p the mass density of the particle ($kg.m^{-3}$), ρ_f the mass density of the fluid ($kg.m^{-3}$), and μ the viscosity ($kg.m^{-1}.s^{-1}$). With this equation, the ~3 μm SS particle population is expected to settle within about 35 min, while the ~0.8 μm particle population would be expected to settle within about 500 min (8 h). The undetectable change in the number of natural colloids in the water column (i.e. no decrease over time) associated with the fast kinetics of SS particle sedimentation, led to the conclusion that homo-aggregation and gravitational settling in the most favorable mechanism of steel particle partitioning in the mesocosms.

3.3.3. Favorable bio-physical-chemical conditions in the planktonic compartment

During the contamination phase, several physical-chemical and microbial parameters were monitored to assess the global response of the mesocosms to the presence of the SS particles in the planktonic compartment. The monitored physical-chemical parameters were constant over the contamination period and close to the those measured on the field the day of sampling (with the exception of the temperature):

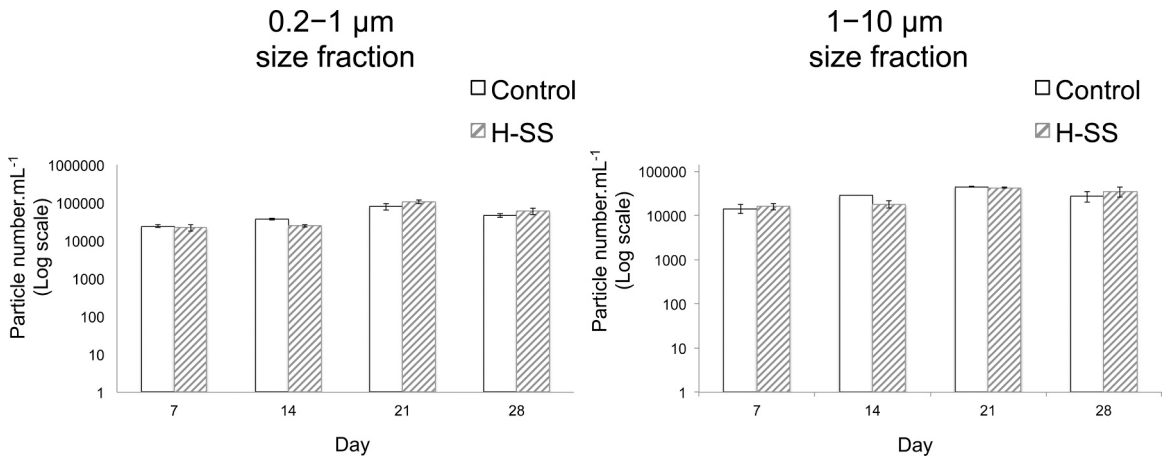

Fig. 4. Number of suspended materials (0.2–1 μm and 1–10 μm) in uncontaminated water from control mesocosms and mesocosms contaminated with steel particles. X-axis: days.

dissolved O_2 (80 −93%, 7 −9 mg.L^{-1}), redox potential (414 ± 72 mV), conductivity (300 ± 4 µS.cm^{-1}), temperature (15.8 ± 0.8 °C), and pH (7.6 ± 0.2) (Fig. S2). The number of picoplankton (cells between 0.2 and 2 µm) measured in the water column at days 0 and 28 remained constant over time, i.e. between 10^4 and 10^5 cells.mL^{-1} (Fig. S3). Moreover, no significant differences were observed between control and contaminated mesocosms, thus no picoplankton mortality resulted from the SS particle exposure.

On the whole, the ecological conditions of the mesocosm water column remained favorable during the exposure to H-SS and T-SS with oxygenation, pH, temperature, redox potential, conductivity, and the number of primary producers all in the range of natural conditions. This is consistent with the selected exposure scenario and the low concentrations measured in the water column, which has been found to be acutely non-toxic for the ecosystem mimicked [43–46].

3.2. Tritiated stainless steel particle accumulation and impacts in the benthic compartment

3.2.1. Tritium and SS behavior and fate in the surficial sediment

Given the relatively low particle stability in the water column, as well as the likelihood of the homo-aggregation scenario discussed above, a significant accumulation in the surficial sediments was expected. In Fig. 5A & 5B, the Mo concentrations determined in the surficial sediment and in its interstitial water were plotted. Despite the large variability attributed to sampling heterogeneity, significant differences in the Mo concentrations measured in the sediment were observed compared to the control at each sampling time. Concentrations averaging between 19 ± 6 mg Mo.kg^{-1} sediment (day 7) and 10 ± 2 mg Mo.kg^{-1} sediment (day 14, 21, and 28) were measured. Given these concentrations, we estimated that at the end of the experiment, 132 ± 37% of the total SS had settled down in the surficial sediment. Similar Mo concentrations (~ 0.6 µg.L^{-1}) in the sediment interstitial water (Fig. 5B) compared to the water column (Fig. 3A & 3B) indicated that the interstitial water was in equilibrium with the water column. Similar results were also obtained for Cr and Ni concentrations, further confirming the settling down of the SS particles in the surficial sediment (Fig. S7).

Regarding the tritium concentration in the benthic compartment, Fig. 5C highlights that the ^{3}H activity in surficial sediment reached 267 ± 57 Bq.mg^{-1} of sediment after 28 days. The ^{3}H activity in the interstitial water of the surficial sediment (Fig. 5D) was also measured and the results (~ 170 Bq.mL^{-1}) obtained at each sampling time again confirmed that the interstitial water was in equilibrium with the water column (Fig. 3D). Two hypotheses can be supported by these results: i) the tritium found in the sediment is still bound to the SS particles, ii) the tritium in the sediment has been first released from the SS particles and then adsorbed at the surface of inorganic or organic phases of the sediment. Assuming that after 28 days in the surficial sediment, all the ^{3}H (267 ± 57 Bq.mg^{-1} of sediment) is still bound to the SS (9.6 ± 1.2 mg Mo.kg^{-1} of sediment), this leads to an estimated particle activity of 0.64 ± 0.14 MBq.mg^{-1} of SS. Taking into consideration the ^{3}H lost to the water column (~16%), this value does not fully represent the expected activity of 0.84 ± 0.2 MBq.mg^{-1} for the SS particles, likely due to the sampling and measurement heterogeneities, but still accounts for an ~80% recovery of ^{3}H and suggests that the first hypothesis is the most favored. All these results highlight that the surficial sediments concentrate the pollution and will be an important sink of incidental tritiated (nano)particles potentially released during nuclear power plant dismantling.

3.2.2. Tritiated stainless steel particle uptake and impacts on freshwater organisms

A. vortex are benthic grazers that eat algae and biofilms at the sediment/water interface. Since the tritiated steel particles are concentrated

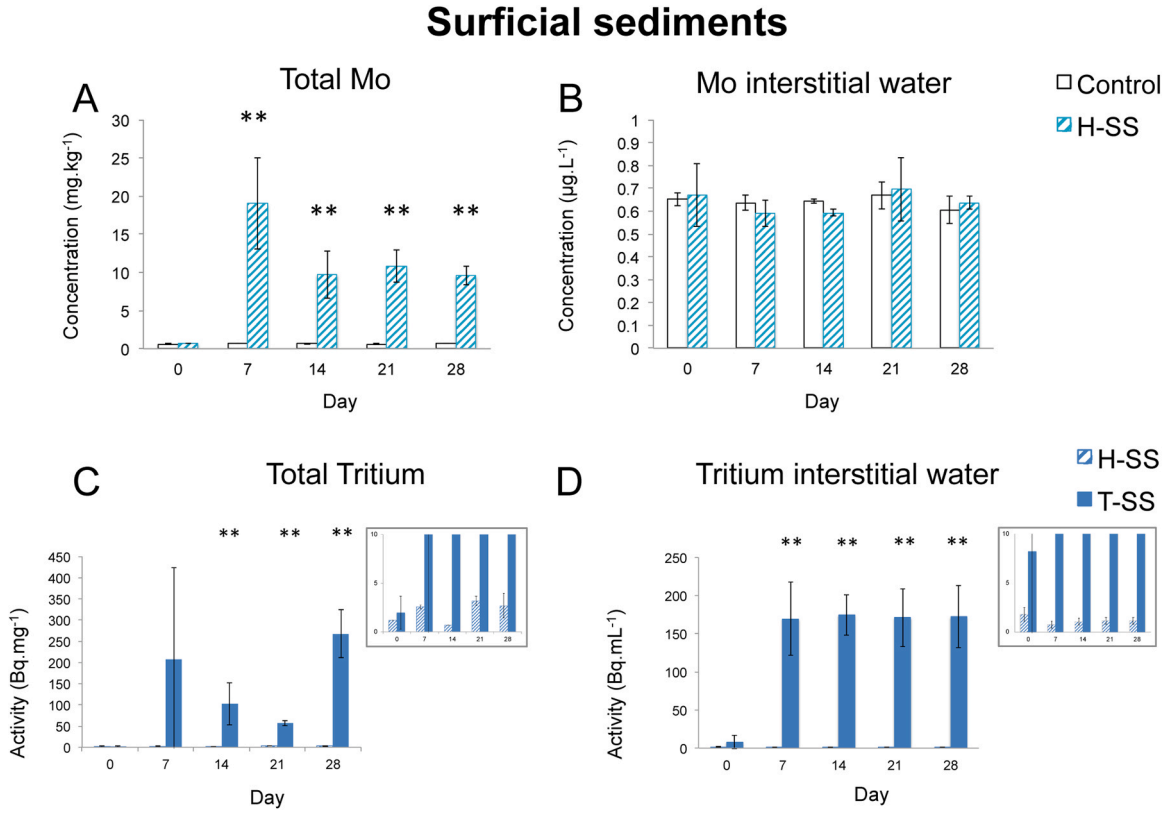

Fig. 5. (A) Mo concentration (mg.kg^{-1}) in surficial sediments and (B) in the interstitial water (µg.L^{-1}) of the control and H-SS exposed mesocosms and (C) ^{3}H activity (Bq.mg^{-1}) in surficial sediments and (D) in the interstitial water (Bq.mL^{-1}) of the H-SS and T-SS exposed mesocosms. Statistical differences between exposed and control mesocosms were evaluated with the Student's t-test; * * $p < 0.05$.

in the sediment, these benthic grazers live and feed in a sensitive ecological niche. The active (ingestion) and passive (adsorption of the shell) uptake of SS particles and ^{3}H was determined by analyzing the elemental content of *A. vortex* before and after rinsing at 14 and 28 days.

Using Mo as the SS tracer, a passive interaction (e.g., adsorption on the shell) between the particles and the snails was observed, with ~0.8 ng of Mo per snail (~0.005% of injected SS particles) measured in the rinse water at day 28. Moreover, a significant Mo concentration (0.22 ± 0.06 mg.kg^{-1}) and ^{3}H activity (4.25 ± 1.36 Bq.mg^{-1}) were measured in the rinsed snails at day 14, suggesting an active uptake (Fig. 6A and 6B). These concentrations at day 14 correspond to $< 0.01\%$ of the SS and $< 0.01\%$ of the ^{3}H initially injected after subtraction of the background of the relevant controls. Assuming that all the ^{3}H taken up is still bound to the SS, this leads to a particle activity of 0.51 ± 0.40 MBq.mg^{-1} of SS. As for the sediment, this value does not fully represent the expected SS particle activity of 0.84 ± 0.2 MBq.mg^{-1} after the initial 16% ^{3}H release in the water column, likely due in this case to a low [Mo] as well as sampling and measurement heterogeneities, but still supports the hypothesis that the ^{3}H taken up remained bound to the SS particles. After 28 days, the concentrations and activity ([Mo] $= 0.16 \pm 0.03$ mg.kg^{-1}, [Ni]$= 0.86 \pm 0.15$ mg.kg^{-1}, [Cr]$= 0.65 \pm 0.23$ mg.kg^{-1}, ^{3}H activity of 4.65 Bq.mg^{-1}) remained constant. Although the measurement of ^{3}H at day 28 only represents the result from one mesocosm due to loss of the replicate sample, this value is consistent with the ^{3}H amount estimated to be found in the snails using Mo as the tracer for the SS particles and assuming that the tritium remains particle-bound. .

Following exposure to H-SS in the surficial sediment, no acute toxicity was observed towards *A. vortex* (<1% of mortality) nor the primary producers (no change in the number of picobenthos ~10^{6} cells. mL^{-1}) over the duration of the experiment (Fig. S3).

Nevertheless, aquatic organisms can respond to stress with a combination of physiological adaptation and behavioral responses [47]. Behavioral modification in animals is one of the most sensitive indicators of environmental stress [48]. Herein, we noticed that *A. vortex* behavior was affected following exposure to the H-SS particles. After 18 and 21 days of exposure, there was a significant increase in the fraction of snails burrowing at the sediment surface, with fractions of 2.2 ± 0.3 and 4.3 ± 0.5, respectively after normalization to controls (Fig. 7). Of note, a fraction of 1.0 indicates no behavioral change with respect to control organisms. Such negative effects on living traits of freshwater snails have already been observed following a decrease in temperature [49], exposure to metals [50] or pesticides [51], and also in the presence of invasive predator populations [52]. These behavioral changes could have implications on the ecology, population dynamics and habitat features of a species [53]. Being less mobile in/at the surface of the sediment, the snails will be more exposed to predators, the interactions between snails will be reduced, and the grazing patterns of snails will be affected, which will impact their feeding regimen, the periphyton

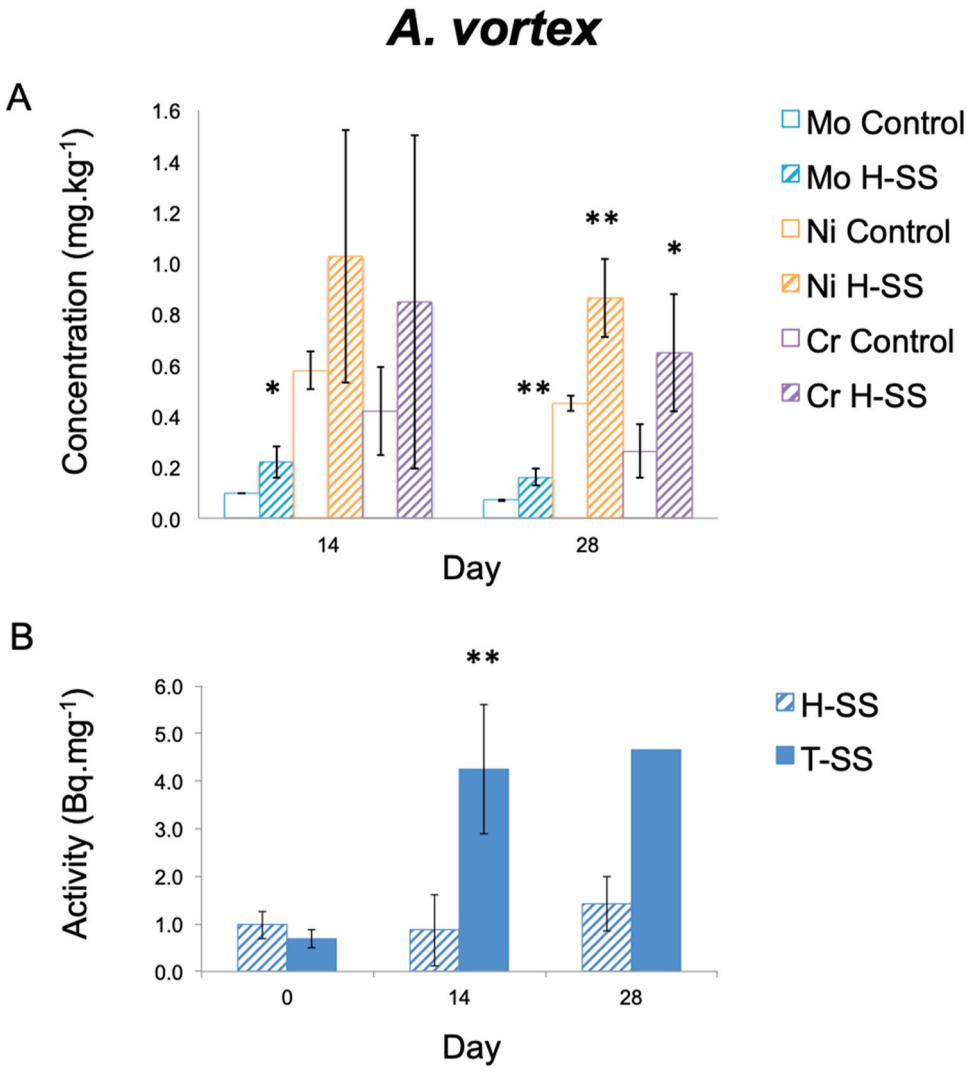

Fig. 6. Concentration of A) metals (mg/kg) and B) ^{3}H activity (Bq/mg) accumulated in *A. vortex*. Statistical differences between exposed and control mesocosms were evaluated with the Student's t-test; * $p < 0.1$, * * $p < 0.05$.

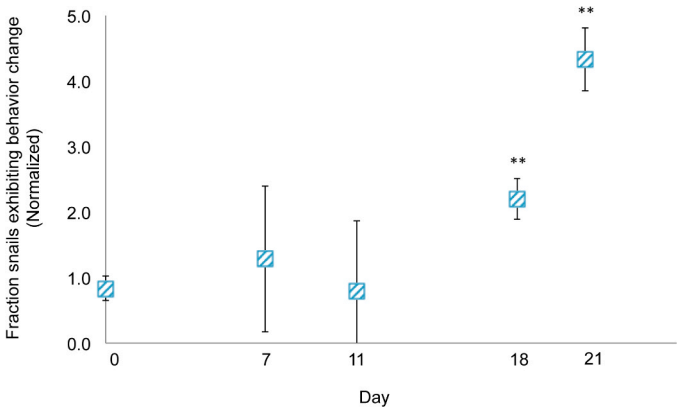

Fig. 7. Fraction of snail population residing at/in sediment surface in H-SS contaminated mesocosms normalized to controls. Statistical differences between exposed and control mesocosms were evaluated with the Student's t-test; * * $p < 0.05$.

communities, and thus the overall balance and health of the freshwater ecosystem [54].

Based on the feeding regimen of the snails and on previous mesocosm experiments performed with TiO_2, CuO and CeO_2 engineered nanoparticles, it is likely that the SS (nano)particles are localized in the digestive gland of *A. vortex* where they undergo enzymatic digestion [43–45,55]. In depth characterization of the localization (at tissular and cellular scale) and speciation of the metals (e.g., Fe, Ni, Cr, Mo) is required to better understand the biodistribution and biotransformation of the SS particles, as well as the bio-physico-chemical mechanisms of toxicity. For instance, the delay of 11–18 days before observing significant changes (Fig. 7) could be attributed to the more or less rapid modification (depending on the group of invertebrates) of the enzymatic systems which regulate behavior (carboxylesterases, glutathione S-transferase, cholinesterase, etc.). These toxicokinetic effects on the sensitivity have already been observed in the case of pesticides [56–60] and would require confirmation for H-SS exposure. Moreover, a thorough characterization of the biological responses in the presence of T-SS is still required. Indeed, with mixtures (as in tritiated stainless steel (nano)particles), we could observe additive effects (e.g., the sum of ^{3}H and metal toxicities), synergistic effects (inducing toxic effects greater than the sum of the effects of the individual chemicals) or also antagonistic effects (where the combined effect of is less toxic than the individual effects) [61,62]. The potential combined radiotoxicity (due to ^{3}H) and particle toxicity (due to SS particles) needs to be further understood.

4. Conclusions

The present indoor freshwater mesocosm experiment permitted the analysis of the environmental fate and impact of anthropogenic tritiated stainless steel (nano)particles and dissolved tritium following a one-time contamination scenario. Our results demonstrated that upon entering the aquatic environment, the stainless steel (nano)particles exhibited no significant solubility, rapidly settled down, and accumulated at the water/sediment interface. During the exposure, ~16% of the tritium was rapidly lost to the water column, while the majority of the tritium (>80%) remained associated to the stainless steel (nano)particles or sediment. Thus, tritium association with or transport by incidental anthropogenic (nano)particles generated during dismantling activities will drive its environmental behavior and fate. The accumulation of stainless steel particles and the associated tritium in the sediment represents a high exposure of the benthic ecological niche. While no acute toxicity was observed towards the picoplanktonic and picobenthic communities or the benthic grazers, the benthic grazers presented significant behavioral changes in the presence of stainless steel particles, exhibiting increased burrowing at the sediment surface despite low steel uptake (<0.01%). This behavior change is an indicator of environmental stress and further studies are thus warranted to understand the mechanisms related to this response, evaluate any combined radiotoxicity and particle toxicity, and confirm if benthic grazer gastropods such as *A. vortex* can be used as indicator species for this type of radioactive particle contamination. Altogether, these results provide some of the first elements of knowledge on the potential dosimetry and environmental impacts of tritiated stainless steel particles, which will allow for improved hazard and risk management.

Funding

This project has received funding from the Euratom Research and Innovation Programme 2014–2018 under grant agreement no. 754586. The views and opinions expressed herein do not necessarily reflect those of the European Commission.

Environmental Implication

Tritiated stainless steel (nano)particles may accidentally be released into freshwater environments during a nuclear facility dismantling incident. These particles, containing radioactive tritium and potentially toxic metals, represent a hazardous material of emerging concern. To date, little is known about the behavior, fate and toxicity of such tritiated particles and it is therefore difficult to anticipate their environmental impacts. The current work helps address this by providing the first elements of knowledge on the dosimetry and particle fate in different environmental compartments, as well as identifying the organisms and ecological niches likely to be exposed, using an environmentally relevant exposure scenario.

CRediT authorship contribution statement

Danielle L. Slomberg: Conceptualization, Data curation, Formal analysis, Investigation, Methodology, Project Administration, Writing – original draft. **Mélanie Auffan:** Conceptualization, Data curation, Formal analysis, Investigation, Methodology, Project Administration, Supervision, Writing – original draft. **Mickaël Payet:** Data curation, Investigation, Methodology, Writing – review & editing. **Andrea Carboni:** Methodology, Investigation. **Amazigh Ouaksel**: Investigation. **Lenka Brousset:** Investigation. **Bernard Angeletti:** Investigation. **Christian Grisolia:** Funding acquisition, Project administration. **Alain Thiéry:** Investigation, Writing – review & editing. **Jérôme Rose:** Conceptualization, Funding acquisition, Project Administration, Supervision, Writing – review & editing.

Declaration of Competing Interest

The authors declare that they have no known competing financial interests or personal relationships that could have influenced the work reported in this paper.

Data Availability

The datasets can be found in the MESOCOSM database platform [https://mesocosmdb.cerege.fr/], as well as the repository Zenodo [https://zenodo.org/record/7255814, DOI: 10.5281/zenodo.7255814].

Acknowledgments

We thank the CNRS for funding the IRP INOVE. The authors thank the Molecular Labeling and Bio-organic Chemistry (SCBM) unit at CEA Paris-Saclay, and in particular Sébastien Garcia-Argote and Cristelle Bisson, for hosting the tritium experiments. We also thank Andrea Campos of Aix-Marseille University/Fédération Sciences Chimiques

Marseille (FSCM) for SEM-EDS imaging and analysis.

Appendix A. Supporting information

Supplementary data associated with this article can be found in the online version at doi:10.1016/j.jhazmat.2023.133093.

References

[1] McCarthy, J., Zachara, J., 1989. ES&T features: subsurface transport of contaminants. Env Sci Technol 23, 496–502. https://doi.org/10.1021/es00063a602.

[2] Penrose, W.R., Polzer, W.L., Essington, E.H., Nelson, D.M., Orlandini, K.A., 1990. Mobility of plutonium and americium through a shallow aquifer in a semiarid region. Env Sci Technol 24, 228–234. https://doi.org/10.1021/es00072a012.

[3] Orlandini, K.A., Penrose, W.R., Harvey, B.R., Lovett, M.B., Findlay, M.W., 1990. Colloidal behavior of actinides in an oligotrophic lake. Env Sci Technol 24, 706–712. https://doi.org/10.1021/es00075a015.

[4] Wigginton, N.S., Haus, K.L., Hochella Jr, M.F., 2007. Aquatic environmental nanoparticles. J Environ Monit 9, 1306–1316. https://doi.org/10.1039/B712709J.

[5] Hochella Jr, M.F., Lower, S.K., Maurice, P.A., Penn, R.L., Sahai, N., Sparks, D.L., Twining, B.S., 2008. Nanominerals, mineral nanoparticles, and earth systems. Science 319, 1631–1635. https://doi.org/10.1126/science.1141134.

[6] Westerhoff, P., Atkinson, A., Fortner, J., Wong, M.S., Zimmerman, J., Gardea-Torresdey, J., Ranville, J., Herckes, P., 2018. Low risk posed by engineered and incidental nanoparticles in drinking water. Nat Nanotechnol 13, 661–669. https://doi.org/10.1038/s41565-018-0217-9.

[7] Makhlaj, V.A., Garkusha, I.E., Aksenov, N.N., Chuvilo, A.A., Chebotarev, V.V., Landman, I., Malykhin, S.V., Pestchanyi, S., Pugachov, A.T., 2013. Dust generation mechanisms under powerful plasma impacts to the tungsten surfaces in ITER ELM simulation experiments. J Nucl Mater 438, S233–S236. https://doi.org/10.1016/j.jnucmat.2013.01.034.

[8] Acsente, T., Negrea, R.F., Nistor, L.C., Logofatu, C., Matei, E., Birjega, R., Grisolia, C., Dinescu, G., 2015. Synthesis of flower-like tungsten nanoparticles by magnetron sputtering combined with gas aggregation. Eur Phys J D 69, 1–7. https://doi.org/10.1140/epjd/e2015-60097-4.

[9] Liger, K., Grisolia, C., Cristescu, I., Moreno, C., Malard, V., Coombs, D., Markelj, S., 2018. Overview of the TRANSAT (TRANSversal Actions for Tritium) project. Fusion Eng Des 136, 168–172. https://doi.org/10.1016/j.fusengdes.2018.01.037.

[10] Sobrido, M.S., Bernard, E., Angeletti, B., Malard, V., George, I., Chaurand, P., Uboldi, C., Orsière, T., Dine, S., Vrel, D., Rousseau, B., 2020. Oxidative transformation of Tungsten (W) nanoparticles potentially released in aqueous and biological media in case of Tokamak (nuclear fusion) Lost of Vacuum Accident (LOVA). Comptes Rendus Géoscience 352, 539–558. https://doi.org/10.5802/crgeos.41.

[11] Decanis, C., Kresina, M., Canas, D., 2018. Methodology to identify appropriate options to manage tritiated waste. Fusion Eng Des 136, 276–281. https://doi.org/10.1016/j.fusengdes.2018.02.008.

[12] Boyer, C., Vichot, L., Fromm, M., Losset, Y., Tatin-Froux, F., Guétat, P., Badot, P.M., 2009. Tritium in plants: A review of current knowledge. Environ Exp Bot 67, 34–51. https://doi.org/10.1016/j.envexpbot.2009.06.008.

[13] Kudryasheva, N.S., Rozhko, T.V., 2015. Effect of low-dose ionizing radiation on luminous marine bacteria: Radiation hormesis and toxicity. J Environ Radioact 142, 68–77. https://doi.org/10.1016/j.jenvrad.2015.01.012.

[14] Nie, B., Fang, S., Jiang, M., Wang, L., Ni, M., Zheng, J., Yang, Z., Li, F., 2021. Anthropogenic tritium: Inventory, discharge, environmental behavior and health effects. Renew Sustain Energy Rev 135, 110188. https://doi.org/10.1016/j.rser.2020.110188.

[15] Bondareva, L., Kudryasheva, N., Tananaev, I., 2022. Tritium: Doses and responses of aquatic living organisms (model experiments). Environments 9, 51. https://doi.org/10.3390/environments9040051.

[16] Kim, S.B., Baglan, N., Davis, P.A., 2013. Current understanding of organically bound tritium (OBT) in the environment. J Environ Radioact 126, 83–91. https://doi.org/10.1016/j.jenvrad.2013.07.011.

[17] Kim, S.B., Shultz, C., Stuart, M., McNamara, E., Festarini, A., Bureau, D.P., 2013. Organically bound tritium (OBT) formation in rainbow trout (*Oncorhynchus mykiss*): HTO and OBT-spiked food exposure experiments. Appl Radiat Isot 72, 114–122. https://doi.org/10.1016/j.apradiso.2012.10.001.

[18] Kim, S.B., Bredlaw, M., Rousselle, H., Stuart, M., 2019. Distribution of organically bound tritium (OBT) activity concentrations in aquatic biota from Eastern Canada. J Environ Radioact 208, 105997. https://doi.org/10.1016/j.jenvrad.2019.105997.

[19] Jaeschke, B.C., Bradshaw, C., 2013. Bioaccumulation of tritiated water in phytoplankton and trophic transfer of organically bound tritium to the blue mussel, Mytilus edulis. J Environ Radioact 115, 28–33. https://doi.org/10.1016/j.jenvrad.2012.07.008.

[20] Jacobs, D.G., 1968. Sources of tritium and its behavior upon release to the environment. AEC Crit Rev Ser. https://doi.org/10.2172/4799828.

[21] Puls, R.W., Powell, R.M., 1992. Transport of inorganic colloids through natural aquifer material: implications for contaminant transport. Env Sci Technol 26, 614–621. https://doi.org/10.1021/es00027a027.

[22] Tran, E., Zavrin, M., Kersting, A.B., Klein-BenDavid, O., Teutsch, N., Weisbrod, N., 2021. Colloid-facilitated transport of 238Pu, 233U and 137Cs through fractured chalk: Laboratory experiments, modelling, and implications for nuclear waste disposal. Sci Total Environ 757, 143818. https://doi.org/10.1016/j.scitotenv.2020.143818.

[23] Midander, K., Pan, J., Leygraf, C., 2006. Elaboration of a test method for the study of metal release from stainless steel particles in artificial biological media. Corros Sci 48, 2855–2866. https://doi.org/10.1016/j.corsci.2005.10.005.

[24] Song, Y.Y., Bhadeshia, H.K.D.H., Suh, D.-W., 2015. Stability of stainless-steel nanoparticle and water mixtures. Powder Technol 272, 34–44. https://doi.org/10.1016/j.powtec.2014.11.026.

[25] Gutierrez, M.F., Ale, A., Andrade, V., Bacchetta, C., Rossi, A., Cazenave, J., 2021. Metallic, metal oxide, and metalloid nanoparticles toxic effects on freshwater microcrustaceans: An update and basis for the use of new test species. Water Environ Res 93, 2505–2526. https://doi.org/10.1002/wer.1637.

[26] Wang, T., Liu, W., 2022. Emerging investigator series: metal nanoparticles in freshwater: transformation, bioavailability and effects on invertebrates. Environ Sci: Nano 9, 2237–2263. https://doi.org/10.1039/D2EN00052K.

[27] Auffan, M., Flahaut, E., Thill, A., Mouchet, F., Carriere, M., Gauthier, L., Achouak, W., Rose, J., Wiesner, M.R., Bottero, J.Y., 2011. Ecotoxicology: Nanoparticle reactivity and living organisms. In *Nanoethics and nanotoxicology*. Springer Berlin Heidelberg,, Berlin, Heidelberg, pp. 325–357.

[28] Vernon, E.L., Jha, A.N., Ferreira, M.F., Slomberg, D.L., Malard, V., Grisolia, C., Payet, M., Turner, A., 2022. Bioaccumulation, release and genotoxicity of stainless steel particles in marine bivalve molluscs. Chemosphere 303, 134914. https://doi.org/10.1016/j.chemosphere.2022.134914.

[29] Praetorius, A., Labille, J., Scheringer, M., Thill, A., Hungerbühler, K., Bottero, J.-Y., 2014. Heteroaggregation of titanium dioxide nanoparticles with model natural colloids under environmentally relevant conditions. Environ Sci Technol 48, 10690–10698. https://doi.org/10.1021/es501655v.

[30] Slomberg, D.L., Ollivier, P., Radakovitch, O., Baran, N., Sani-Kast, N., Miche, H., Borschneck, D., Grauby, O., Bruchet, A., Scheringer, M., Labille, J., 2016. Characterisation of suspended particulate matter in the Rhone River: Insights into analogue selection. Environ Chem 13, 804–815. https://doi.org/10.1071/EN15065.

[31] Slomberg, D.L., Ollivier, P., Miche, H., Angeletti, B., Bruchet, A., Philibert, M., Brant, J., Labille, J., 2019. Nanoparticle stability in lake water shaped by natural organic matter properties and presence of particulate matter. Sci Total Environ 656, 338–346. https://doi.org/10.1016/j.scitotenv.2018.11.279.

[32] Joo, S.H., Zhao, D., 2017. Environmental dynamics of metal oxide nanoparticles in heterogeneous systems: A review. J Hazard Mater 322, 29–47. https://doi.org/10.1016/j.jhazmat.2016.02.068.

[33] Bour, A., Mouchet, F., Silvestre, J., Gauthier, L., Pinelli, E., 2015. Environmentally relevant approaches to assess nanoparticles ecotoxicity: A review. J Hazard Mater 283, 764–777. https://doi.org/10.1016/j.jhazmat.2014.10.021.

[34] Carboni, A., Slomberg, D.L., Nassar, M., Santaella, C., Masion, A., Rose, J., Auffan, M., 2021. Aquatic mesocosm strategies for the environmental fate and risk assessment of engineered nanomaterials. Environ Sci Technol 55, 16270–16282. https://doi.org/10.1021/acs.est.1c02221.

[35] Auffan, M., Tella, M., Santaella, C., Brousset, L., Paillès, C., Barakat, M., Espinasse, B., Artells, E., Issartel, J., Masion, A., Rose, J., Wiesner, M.R., Achouak, W., Thiéry, A., Bottero, J.-Y., 2014. An adaptable mesocosm platform for performing integrated assessments of nanomaterial risk in complex environmental systems. Sci Rep 4, 5608. https://doi.org/10.1038/srep05608.

[36] Gensdarmes, F.; Payet, M.; Malard, V.; Grisolia, C., Report on production of steel particles, TRANSAT Deliverable 3.1, Horizon 2020 Programme, (2019). ⟨https://transat-h2020.eu/wp-content/uploads/2020/04/TRANSAT-D3.1-Report-on-Production-of-Steel-Particles.pdf⟩.

[37] Payet, M.; Report on tritiation of cement and steel particles, TRANSAT Deliverable 3.3, Horizon 2020 Programme, (2020). ⟨https://transat-h2020.eu/wp-content/uploads/2020/04/TRANSAT-D3.3-Report-on-tritiation-of-cement-and-steel-particles.pdf⟩.

[38] Sanchez, W., Porcher, J.-M., 2009. Fish biomarkers for environmental monitoring within the water framework directive of the European Union. TrAC Trends Anal Chem 28, 150–158. https://doi.org/10.1016/j.trac.2008.10.012.

[39] Shinn, C., Impact of toxicants on stream fish biological traits, Doctoral dissertation - Université de Toulouse, Université Toulouse III-Paul Sabatier, 2010.

[40] Matsuyama, M., Chen, Z., Nisimura, K., Akamaru, S., Torikai, Y., Hatano, Y., Ashikawa, N., Oya, Y., Okuno, K., Hino, T., 2011. Trapping and depth profile of tritium in surface layers of metallic materials. J Nucl Mater 417, 900–903. https://doi.org/10.1016/j.jnucmat.2011.04.005.

[41] Sharpe, M., Fagan, C., Shmayda, W.T., 2019. Distribution of tritium in the near surface of type 316 stainless steel. Fusion Sci Technol 75, 1053–1057. https://doi.org/10.1080/15361055.2019.1644136.

[42] Lamb, H., 1932. Hydrodynamics, 6th ed..,. Cambridge University Press,.

[43] Tella, M., Auffan, M., Brousset, L., Morel, E., Proux, O., Chanéac, C., Angeletti, B., Pailles, C., Artells, E., Santaella, C., Rose, J., Thiéry, A., Bottero, J.-Y., 2015. Chronic dosing of a simulated pond ecosystem in indoor aquatic mesocosms: Fate and transport of CeO_2 nanoparticles. Environ Sci Nano 2, 653–663. https://doi.org/10.1039/C5EN00092K.

[44] Tella, M., Auffan, M., Brousset, L., B, Issartel, J., Kieffer, I., Pailles, C., Morel, E., Santaella, C., Angeletti, B., Artells, E., Rose, J., Thiéry, A., Bottero, J.-Y., 2014. Transfer, transformation, and impacts of ceria nanomaterials in aquatic mesocosms simulating a pond ecosystem. Environ Sci Technol 48, 9004–9013. https://doi.org/10.1021/es501641b.

[45] Châtel, A., Auffan, M., Perrein-Ettajani, H., Brousset, L., Métais, I., Chaurand, P., Mouloud, M., Clavaguera, S., Gandolfo, Y., Bruneau, M., Masion, A., Thiéry, A., Rose, J., Mouneyrac, C., 2020. The necessity of investigating a freshwater-marine continuum using a mesocosm approach in nanosafety: The case study of TiO_2

MNM-based photocatalytic cement. NanoImpact 20, 100254. https://doi.org/10.1016/j.impact.2020.100254.
[46] Auffan, M., Santaella, C., Brousset, L., Tella, M., Morel, E., Ortet, P., Barakat, M., Chaneac, C., Issartel, J., Angeletti, B., Levard, C., Hazemann, J.-L., Wiesner, M., Rose, J., Thiéry, A., Bottero, J.-Y., 2020. The shape and speciation of Ag nanoparticles drive their impacts on organisms in a lotic ecosystem. Environ Sci Nano 7, 3167–3177. https://doi.org/10.1039/D0EN00442A.
[47] MacInnes, J.R., Thurberg, F.P., 1973. Effects of metals on the behaviour and oxygen consumption of the mud snail. Mar Pollut Bull 4, 185–186. https://doi.org/10.1016/0025-326X(73)90225-7.
[48] Eisler, R., Carney, G.C., Lockwood, A.P.M., Perkins, E.J., Cole, H.A., 1997. Behavioural responses of marine poikilotherms to pollutants. Philos Trans R Soc Lond B Biol Sci 286, 507–521. https://doi.org/10.1098/rstb.1979.0043.
[49] Buerger, H., 1975. Movement and burrowing of *Helisoma Trivolvis* (Say) (Gastropoda, Planorbidae) in a Small Pond. Can J Zool 53, 456–464. https://doi.org/10.1139/z75-059.
[50] Kamble, S.B., Kamble, N.A., 2014. Behavioural changes in freshwater snail *Bellamya Bengalensis* due to acute toxicity of copper sulphate and *Acacia Sinuata*, Int. J. Sci. Environ Technol 3, 1090–1104.
[51] Elias, D., Bernot, M.J., 2017. Effects of individual and combined pesticide commercial formulations exposure to egestion and movement of common freshwater snails, *Physa Acuta* and *Helisoma anceps*. Am Midl Nat 178, 97–111. https://doi.org/10.1674/0003-0031-178.1.97.
[52] Levri, E.P., Berkheimer, C., Wilson, K., Xu, J., Woods, T., Hutchinson, S., Yoder, K., Zhang, X., Li, X., 2020. The cost of predator avoidance behaviors in an invasive freshwater snail. Freshw Sci 39, 476–484. https://doi.org/10.1086/710107.
[53] Lillebø, A.I., Pardal, M.Â., Marques, J.C., 1999. Population structure, dynamics and production of *Hydrobia ulvae* (Pennant) (Mollusca: Prosobranchia) along an eutrophication gradient in the Mondego Estuary (Portugal). Acta Oecologica 20, 289–304. https://doi.org/10.1016/S1146-609X(99)00137-X.
[54] Burris, J.A., Bamford, M.S., Stewart, A.J., 1990. Behavioral responses of marked snails as indicators of water quality. Environ Toxicol Chem 9, 69–76. https://doi.org/10.1002/etc.5620090109.
[55] Auffan, M., Liu, W., Brousset, L., Scifo, L., Pariat, A., Sanles, M., Chaurand, P., Angeletti, B., Thiery, A., Masion, A., Rose, J., 2018. Environmental Exposure of a Simulated Pond Ecosystem to CuO Nanoparticle Based-Wood Stain throughout Its Life Cycle. Environ Sci Nano 5, 2579–2589. https://doi.org/10.1039/C7EN00494J.
[56] Martínez Morcillo, S., Yela, J.L., Capowiez, Y., Mazzia, C., Rault, M., Sanchez-Hernandez, J.C., 2013. Avoidance behaviour response and esterase inhibition in the earthworm, *Lumbricus Terrestris*, after exposure to chlorpyrifos. Ecotoxicology 22, 597–607. https://doi.org/10.1007/s10646-013-1051-3.
[57] Otero, S., Kristoff, G., 2016. In vitro and in vivo studies of cholinesterases and carboxylesterases in *Planorbarius Corneus* exposed to a phosphorodithioate insecticide: Finding the most sensitive combination of enzymes, substrates, tissues and recovery capacity. Aquat Toxicol 180, 186–195. https://doi.org/10.1016/j.aquatox.2016.10.002.
[58] Jouni, F., Sanchez-Hernandez, J.C., Mazzia, C., Jobin, M., Capowiez, Y., Rault, M., 2018. Interspecific differences in biochemical and behavioral biomarkers in endogeic earthworms exposed to ethyl-parathion. Chemosphere 202, 85–93. https://doi.org/10.1016/j.chemosphere.2018.03.060.
[59] Jouni, F., Sanchez-Hernandez, J.C., Brouchoud, C., Capowiez, Y., Rault, M., 2023. Role of soil texture and earthworm casts on the restoration of soil enzyme activities after exposure to an organophosphorus insecticide. Appl Soil Ecol 187, 104840. https://doi.org/10.1016/j.apsoil.2023.104840.
[60] Sedeño-Díaz, J.E., López-López, E., 2022. Oxidative stress in *Physella acuta*: An integrative response of exposure to water from two rivers of Atlantic Mexican Slope. Front Physiol 13, 1805. https://doi.org/10.3389/fphys.2022.932537.
[61] Roell, K.R., Reif, D.M., Motsinger-Reif, A.A., 2017. An introduction to terminology and methodology of chemical synergy—Perspectives from across disciplines. Front Pharmacol 8, 158. https://doi.org/10.3389/fphar.2017.00158.
[62] Li, M., Liu, W., Slaveykova, V.I., 2020. Effects of mixtures of engineered nanoparticles and metallic pollutants on aquatic organisms. Environments 7, 27. https://doi.org/10.3390/environments7040027.